Voltage-Controlled Dzyaloshinskii-Moriya Interaction Torque Switching of Perpendicular Magnetization

Dongxing Yu,[1,3] Yonglong Ga,[3] Jinghua Liang,[3] Chenglong Jia●,[2,*] and Hongxin Yang●[1,3,†]

[1]*National Laboratory of Solid State Microstructures, School of Physics,*
Collaborative Innovation Center of Advanced Microstructures, Nanjing University, Nanjing 210093, China
[2]*Key Laboratory for Magnetism and Magnetic Materials of MOE and Lanzhou Center for Theoretical Physics,*
Lanzhou University, Lanzhou 730000, China
[3]*Ningbo Institute of Materials Technology and Engineering, Chinese Academy of Sciences, Ningbo 315201, China*

Magnetization switching is the most important operation in spintronic devices. In modern nonvolatile magnetic random-access memory (MRAM), it is usually realized by spin-transfer torque (STT) or spin-orbit torque (SOT). However, both STT and SOT MRAM require current to drive magnetization switching, which will cause Joule heating. Here, we report an alternative mechanism, Dzyaloshinskii-Moriya interaction (DMI) torque, that can realize magnetization switching fully controlled by voltage pulses. We find that a consequential voltage-controlled reversal of DMI chirality in multiferroics can lead to continued expansion of a skyrmion thanks to the DMI torque. Enough DMI torque will eventually make the skyrmion burst into a quasiuniform ferromagnetic state with reversed magnetization, thus realizing the switching of a perpendicular magnet. The discovery is demonstrated in two-dimensional multiferroics, CuCrP$_2$Se$_6$ and CrN, using first-principles calculations and micromagnetic simulations. As an example, we applied the DMI torque for simulating leaky-integrate-fire functionality of biological neurons. Our discovery of DMI torque switching of perpendicular magnetization provides tremendous potential toward magnetic-field-free and current-free spintronic devices, and neuromorphic computing as well.

In conventional semiconductor-based electronics, the current switching is controlled by the on/off ratio of a *p-n* junction to enable information processing. In spintronics, the on/off ratio is realized by the giant or tunneling magnetoresistance effects [1–6] which have dramatically improved the reading efficiency of magnetic memory and storage devices. However, the magnetization switching that is at the core of various spintronic devices, especially for the writing operation, is still a major challenge. Several methods to switch magnetization by means of current-induced spin-transfer torque [7–12] or spin-orbit torque [13–23] have led to the development of modern nonvolatile magnetic random-access memory (MRAM) [9,24–28]. A vital and challenging question is how to effectively control magnetization in a more energy-efficient way. To reduce the power dissipation due to Ohmic conduction, the control of magnetization by using current-free methods [29–41] is highly desired for practical applications.

The Dzyaloshinskii-Moriya interaction (DMI) [42,43], which arises from spin-orbit coupling (SOC) in magnets with inversion symmetry breaking [44–52], plays an essential role in the formation of noncollinear spin textures such as chiral domain walls [53–56] and magnetic skyrmions [57–65]. The torque from DMI can be written as $\boldsymbol{\tau}_{\mathrm{DMI}} = \mathbf{M} \times \mathbf{B}_{\mathrm{DMI}}$, with the effective field $\mathbf{B}_{\mathrm{DMI}}$ obtained

from the functional derivative of DMI energy $E_{\mathrm{DMI}} = \sum_{i,j} -\mathbf{d}_{ij} \cdot (\mathbf{m}_i \times \mathbf{m}_j)$, where $\mathbf{m}$ represents the unit vector of the magnetic moment $\mathbf{M}$ and $\mathbf{d}_{ij} = D(\mathbf{z} \times \mathbf{r}_{ij})$ is the corresponding DMI vector [58,66]. For a skyrmion structure described by $\mathbf{m}_{\mathbf{r}} = [\cos(v\phi + Q_h)\sin\Theta_r, \sin(v\phi + Q_h)\sin\Theta_r, \cos\Theta_r]$ in the polar coordinates r and ϕ, the phase of helicity Q_h is determined by the DMI and can take different values (e.g., $Q_h = 0, \pm\pi/2$, and π) to characterize the spin swirling direction of the skyrmion [67]. v represents the vorticity number ($v = 1$ for a skyrmion and $v = -1$ for an antiskyrmion).

When the sign of DMI in magnetoelectric multiferroics is reversed by a voltage pulse, the micromagnetic energy in a skyrmion will surge, leading to the expansion of the skyrmion and the reversal of skyrmion chirality ($\cos Q_h$) [from Fig. 1(a) to 1(b), and from Fig. 1(d) to 1(e), respectively]. If an opposite voltage pulse following the former one is applied to reverse the sign of DMI before the skyrmion relaxes back to its ground state, the chirality of the skyrmion will be reversed again, causing the skyrmion to expand further [from Fig. 1(b) to 1(c), and from Fig. 1(e) to 1(f), respectively]. This concept of skyrmion expansion induced by the DMI torque is universally valid in structures that can create magnetic skyrmion with reversible chirality, and will be demonstrated by using first-principles calculations and simulations in the following. Based on this
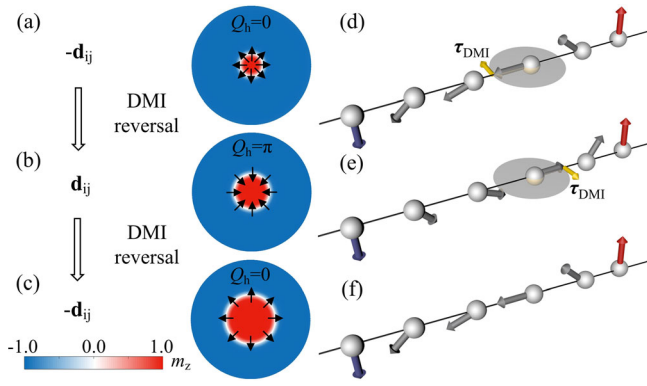
FIG. 1. (a)–(c) Skyrmion expansion due to the sign reversal of DMI. Left: the sign of DMI is reversed from negative (a) to positive (b) and to negative (c). Right: a skyrmion with helicity phase $Q_h = 0$ created initially with DMI vector $-\mathbf{d}_{ij}$ (a), expanded skyrmion with $Q_h = \pi$ due to the sign reversal of DMI vector from $-\mathbf{d}_{ij}$ to $\mathbf{d}_{ij}$ (b), further expanded skyrmion with $Q_h = 0$ due to the continued reversal of DMI vector from $\mathbf{d}_{ij}$ to $-\mathbf{d}_{ij}$ (c). (d)–(f) Sketches of the skyrmion chirality switching corresponding to (a)–(c), respectively. The yellow arrows represent DMI torque $\boldsymbol{\tau}_{\mathrm{DMI}}$.

FIG. 2. (a) Top view of the crystal structure of $CuCrP_2Se_6$. (b) Schematic of polarization switching of $CuCrP_2Se_6$ controlled by a voltage pulse, the sign reversal of DMI (coefficient D) and hence the transformation of magnetic skyrmions between $(Q = 1/-1, Q_h = 0/\pi)$ and $(Q = 1/-1, Q_h = \pi/0)$. (c) Spin spiral energy $E[q]$ and DMI energy $\Delta E_{\mathrm{DMI}}[q]$ for $CuCrP_2Se_6$ with up (blue hollow dotted lines) and down polarization (red solid dotted lines) calculated as a function of spin spiral vector $\mathbf{q}$. Ferromagnetic state is represented at $q = 0$.

mechanism, we propose using voltage-controlled DMI torque to achieve magnetic-field-free and current-free switching of perpendicular magnetization. In a multiferroic film, such as monolayer of $CuCrP_2Se_6$ [68] or CrN [69], a voltage pulse can switch its polarization, hence switching the chirality of DMI [51,70]. Then the sign reversal of DMI will create a torque which can cause the skyrmion expansion. More interestingly, a series of consecutive voltage pulses can continuously expand the skyrmion size. Eventually, enough DMI torque will make the skyrmion burst into a quasiuniform ferromagnetic (FM) state [56,71] in the same direction as its core polarity, resulting in a complete perpendicular magnetization switching of FM background. Unlike the FM state in the absence of DMI, the spins in the quasiuniform FM state are tilted inward or outward at the edges of the nanodot to lower the DMI energy. As an example of possible applications, we demonstrate that the DMI torque switching of perpendicular magnetization can be used to imitate the leaky-integrate-fire (LIF) functionality [72] of biological neurons in neuromorphic computing [73–77]. The proposed mechanism for achieving perpendicular magnetization switching that is completely induced by the voltage-controlled DMI torque avoids the application of electric current or magnetic field and provides promising candidates for next-generation energy-efficient MRAM and neuromorphic computing.

In order to explore the switching mechanism of perpendicular magnetization induced by the voltage-controlled DMI torque, we first take multiferroic $CuCrP_2Se_6$ monolayer [68,78,79] as an example [Figs. 2(a) and 2(b)]. The energy density E of this magnetic system can be written as

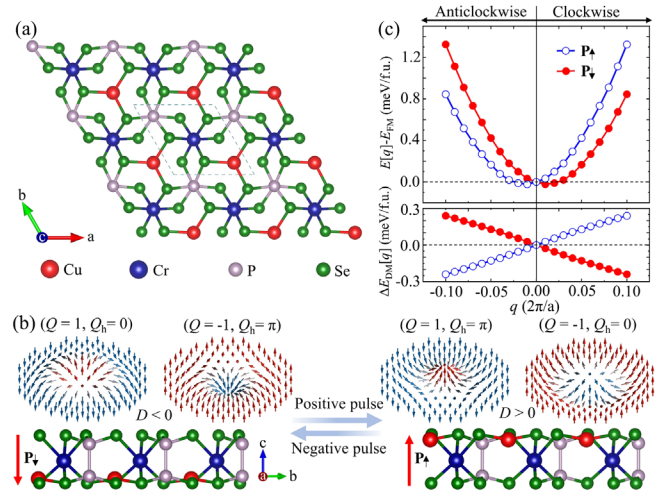$$E = A(\nabla \mathbf{m})^2 - K_u m_z^2 - \frac{1}{2}\mu_0 M_s \mathbf{m} \cdot \mathbf{H}_d$$
$$+ D[m_z(\nabla \cdot \mathbf{m}) - (\mathbf{m} \cdot \nabla)m_z], \qquad (1)$$

where A and K_u are the exchange stiffness and anisotropy energy constant, respectively. $\mathbf{H}_d$ is the magnetostatic self-interaction field. D represents the DMI constant which can be reversed from a negative value to a positive one by a voltage pulse (or electric field), and vice versa (see Fig. S1 in Supplemental Material [80]). For a thin magnetic layer, the K_u and $\mathbf{H}_d$ terms can be included in an effective anisotropy $K = K_u - \mu_0 M_s^2/2$.

As illustrated in Figs. 2(a) and 2(b), the electric polarization of the $CuCrP_2Se_6$ monolayer is determined by the position of the Cu atom. When a vertical positive voltage pulse is applied, the polarization will be reversed from down to up, with the Cu atoms (red balls) being shifted from the bottom side to the top side, and vice versa for the negative voltage case. Figure 2(c) shows the first-principles calculated spin spirals energy $E[q]$ and the resulting DMI energy $\Delta E_{\mathrm{DMI}}[q]$ as a function of spin spiral vector $\mathbf{q}$ for the $CuCrP_2Se_6$ monolayer with the up or down polarization. The slope of $\Delta E_{\mathrm{DMI}}[q]$ shows that the up polarization favors anticlockwise DMI, while down polarization prefers clockwise DMI. Moreover, the atomic resolved SOC energy ΔE_{SOC} associated to DMI (see Fig. S2 in Supplemental Material [80]) further demonstrates that the ΔE_{SOC} of a given atom changes its sign as the polarization is reversed. This will allow the chirality
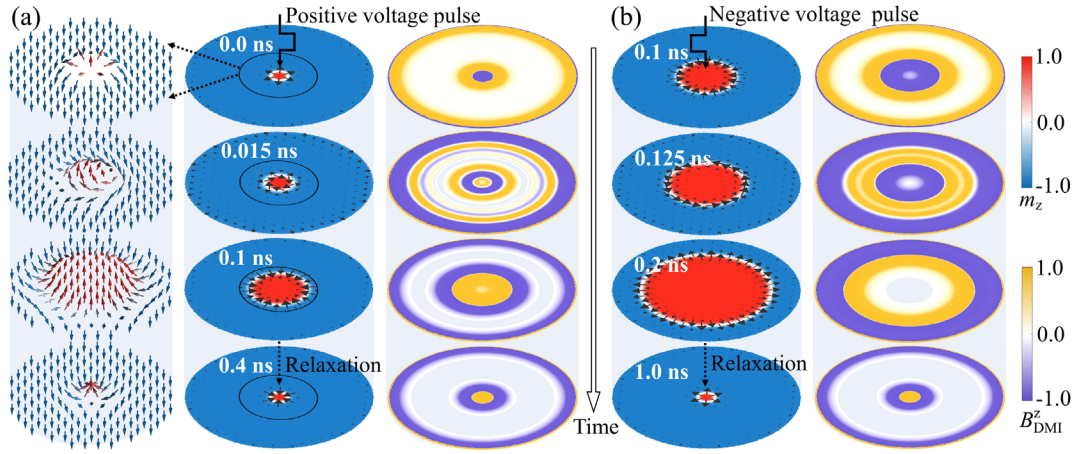
FIG. 3. (a) Snapshots of dynamics of a skyrmion and the distribution of the DMI effective field B_{DMI}^z corresponding to the evolving magnetic skyrmion when a positive voltage pulse is applied from 0 to 0.1 ns at initially 0.0 ns (clockwise Néel-type with helicity phase $Q_h = 0$), 0.015 ns (intermediate Bloch-type with $Q_h = -\pi/2$), 0.1 ns (expanded anticlockwise Néel-type with $Q_h = \pi$), and 0.4 ns (final anticlockwise Néel-type with $Q_h = \pi$), respectively. After the voltage pulse is released at 0.1 ns, the skyrmion relaxes back to its initial size within 0.3 ns. (b) An alternating negative voltage pulse is applied from 0.1 to 0.2 ns in order to further expand the skyrmion. This process is induced by another sign reversal of DMI with a negative voltage pulse that follows the positive one in (a) (at 0.1 ns).

of a skyrmion to be reversibly controlled by voltage. Figure 2(b) shows four skyrmions with different topological properties, which can be described by topological charge $Q = 1/4\pi \int \mathbf{m} \cdot (\partial_x \mathbf{m} \times \partial_y \mathbf{m}) dx dy$ and helicity phase Q_h [67]. The presence of both magnetization and electric polarization in multiferroics, e.g., $CuCrP_2Se_6$, provides us with the unique opportunity for the effective electric control of the chirality of DMI, and thereby the DMI torque switching of perpendicular magnetization.

When a positive voltage pulse from 0 to 0.1 ns is applied to the multiferroic $CuCrP_2Se_6$ monolayer, the helicity of the skyrmion can be reversed from clockwise (Néel-type $Q_h = 0$ at 0 ns) to anticlockwise (Néel-type $Q_h = \pi$ at 0.1 ns) due to the sign reversal of DMI, as shown in Fig. 3(a), left-hand side, from 0 to 0.1 ns. More interestingly, during the reversal process, we also find that the skyrmion performs an obvious expansion of its size [Fig. 3(a), two left-hand panels, and Video Part I in Supplemental Material [80]], which is quite similar to the breathing mode of a skyrmion [95–99] excited by the out-of-plane alternating current magnetic field of microwave, spin current, etc. A sequential voltage pulse would enable the DMI and helicity to switch repeatedly, leading to the accumulation of multiple expansions.

To obtain a full picture of the expansion mechanism, we solve the skyrmion dynamics based on the Landau-Lifshitz-Gilbert equation [90–92,94]. Given that the polar angle $\Theta(r) = 2 \arctan[\sinh(R/w)/\sinh(r/w)]$, where R defines the skyrmion size as $m_z(R) = 0$ and $w = \pi|D|/4K$ is the wall width of the outer domain, the integral DMI energy of the Néel skyrmion then reads

$$E_{\mathrm{DMI}}(R, Q_h) = -2\pi^2 DR \cos Q_h. \tag{2}$$

Thus, we have $Q_h = 0 \ (\pi)$ for $D > 0 \ (<0)$. Consequently, during the sign reversal process of DMI, to lower the energy $E_{\mathrm{DMI}}(R, Q_h)$ via an energy dissipation, we would expect not only the rotational deformations of the outer domain wall but also the expansion of skyrmion size R (see Fig. S3 in Supplemental Material [80]). From the Landau-Lifshitz-Gilbert equation, R is found to be expanded indeed (more details in Supplemental Material [80]):

$$\delta R(t) = 2\frac{w}{\alpha} \operatorname{atan}\left(\tanh \frac{t}{2\tau}\right), \tag{3}$$

with $1/\tau \approx \pi|D|\alpha\gamma/4$. Note that the motion $\delta R(t)$ and the spin-flip time τ are all independent of the core polarization of the skyrmion and the chirality of the outer domain wall, which give rise to the accumulation effect of skyrmion expansion, regardless of its topological charge, vorticity, and helicity. Then, the expansion area δS of a skyrmion is easily gotten:

$$\delta S = \frac{\pi^2 w}{\alpha}\left(2R_0 + \frac{\pi w}{\alpha}\right), \tag{4}$$

where R_0 is the radius of the initial skyrmion. Different from the previous progress in controlling magnetism [30,31,93,100–103] by relying on the direction of the voltage-controlled (or electric-field-controlled) exchange bias, magnetic anisotropy, rolling-downhill-like motion of the domain wall, etc., the magnetic skyrmion and antiskyrmion can be controlled uninterruptedly under the action of the sequential voltage pulses (see Fig. 4 herein and Fig. S4 in Supplemental Material [80]), providing a new topological-soliton-mediated magnetization switching
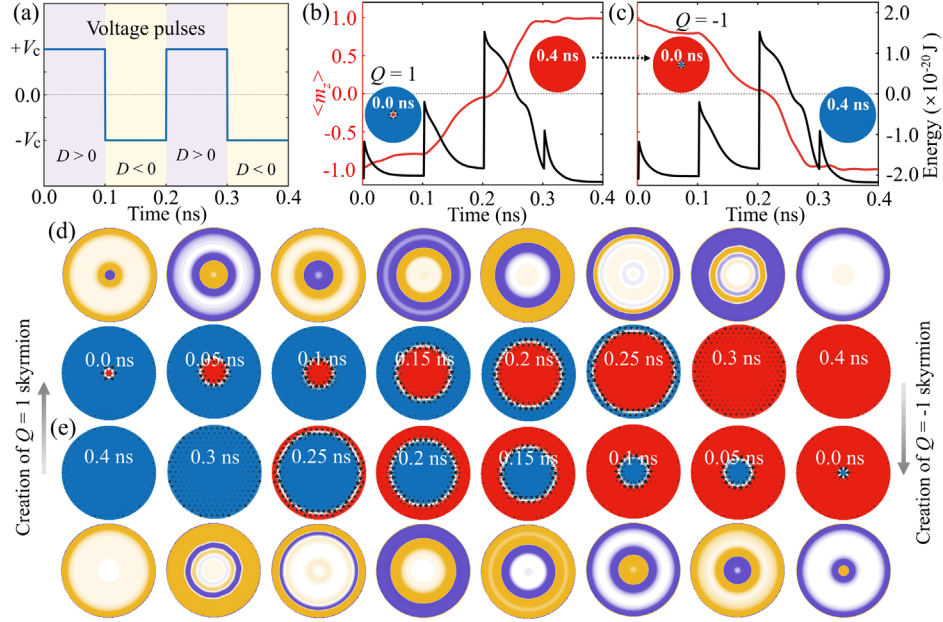
FIG. 4. (a) Alternating sequential voltage pulses used in perpendicular magnetization switching. DMI sign in CuCrP$_2$Se$_6$ will be reversed with the reversal of voltage pulses. (b) Perpendicular magnetization $\langle m_z \rangle$ switching (red line) due to the skyrmion's expansion accumulation for $Q = 1$ case. The sign reversal of DMI leads to an instantaneous surge in micromagnetic energy (black line), indicating a continuous expansion of skyrmion by DMI torque until the skyrmion is annihilated at 0.3 ns. (c) Reverse switching of perpendicular magnetization (red line) by the sequential voltage pulses as in (a), which starts from the skyrmion with a topological charge $Q = -1$. Snapshots of dynamics of the skyrmion in (d) (lower panel) and (e) (upper panel) corresponding to the perpendicular magnetization switching in (b) and (c), respectively. The distribution of DMI effective fields B^z_{DMI} is also shown in (d) and (e), respectively.

mechanism for ferromagnetic systems and even antiferromagnetic systems.

Figure 3(a), right-hand panel, shows the simulated out-of-plane component of the DMI effective field B^z_{DMI} corresponding to the evolving skyrmion as shown in the middle part. When the chirality of the DMI is reversed from clockwise ($D < 0$) to anticlockwise ($D > 0$) by a positive voltage pulse, the DMI effective field B^z_{DMI} around the skyrmion will be opposite to the magnetizations and leads to the expansion of the skyrmion. When the chirality of the skyrmion is completely reversed by the DMI torque, the DMI effective field B^z_{DMI} will also be reversed as shown in Fig. 3(a) at 0.1 ns, and thus prompts the skyrmion to return to its initial size. However, if a negative voltage pulse is applied at 0.1 ns following the positive one, the skyrmion will expand further, forming the expansion accumulation of the skyrmion as shown in Fig. 3(b) (see also Video Part II in Supplemental Material [80]). This is due to the sign of DMI being reversed to a negative value (from $+D$ to $-D$) again under the application of the second negative voltage pulse. When the first positive voltage pulse is released at 0.1 ns, the chirality of the skyrmion has been completely reversed, but the size of it is still in the expansion stage. At this time, the DMI effective field (or DMI torque), which is induced by the second opposite voltage pulse, would trigger the second expansion process [Fig. 3(b), right-hand part].

After reversing the chirality of a skyrmion twice within the first two opposite voltage pulses [Fig. 4(a)], the skyrmion will reach a larger size at 0.2 ns. Then, if a further voltage pulse opposite to the second one is applied, the DMI torque induced by the third reversal of DMI will lead to further expansion of the skyrmion until it bursts into a quasiuniform FM state [Fig. 4(d) herein and Video Part III in Supplemental Material [80]]. Significantly different from the traditional magnetic skyrmion annihilation mode, the direction of the magnetization in the final FM state is opposite to that of the initial state, resulting in the switching of the perpendicular magnetization [Fig. 4(b)]. To perform a reproducible perpendicular magnetization switching, it is necessary to stimulate a new skyrmion which will have opposite topological charge via the techniques such as local heating [104] or spin-polarized current [56]. Hence, the perpendicular magnetization can be switched again [Figs. 4(c) and 4(e) herein and Video Part IV [80]] by DMI torque through the same operation process.

Figure S5 in Supplemental Material [80] shows the response of perpendicular magnetization and skyrmion to the reversal of DMI in a CrN nanodisk. The DMI torque-induced expansion of the skyrmion and perpendicular magnetization switching (see also Video Parts V and VI [80]), which are similar to the skyrmion dynamics in a CuCrP$_2$Se$_6$ nanodisk, further verify the universal applicability of our proposal. The voltage-controlled DMI

torque switching of perpendicular magnetization in our Letter is a conceptually novel mechanism that is intrinsically present, and its existence can also be verified by the atomistic spin dynamics simulations for $CuCrP_2Se_6$ and CrN as shown in Fig. S6 [80]. Moreover, inspired by the behavior of biological neurons and the aforementioned expansion accumulation of a skyrmion, one can imitate the LIF functionality [72] of biological neurons by DMI torque (see Fig. S7 in Supplemental Material [80]) and provide a promising candidate for the magnetic-field-free and current-free manipulation of artificial neurons [73–77].

For realizing the continuous expansion of a skyrmion, the duration of the voltage pulses should be longer than the time required for the chirality reversal of a skyrmion, but the separation should be shorter than the relaxation time required for the skyrmion to return to its initial size (more details can be found in Supplemental Material [80]). In addition, we also find that the magnetization switching is easier to achieve as the temperature increases due to the thermal fluctuation (see Fig. S8 in Supplemental Material [80]), but the switching process becomes no longer stable at high temperatures. Finally, although the above work was done with the Gilbert damping constant $\alpha = 0.2$, the expansion mechanism of the magnetic skyrmion is more pronounced with a smaller damping constant (see Fig. S9 in Supplemental Material [80]).

Controlling magnetism using voltage has a long history, such as the magnetization switching in $BiFeO_3$-based heterostructures [32,100] and antiferromagnetic-ferromagnetic-ferroelectric multiferroic heterostructures [101,102] by exploiting the static magnetoelectric coupling, the switching of topological magnetic structures by virtue of the voltage control of magnetic anisotropy [105], piezoelectric effect [106], etc. However, the expansion effect of a skyrmion solely induced by the reversal of DMI chirality in this Letter has competitive advantage in energy consumption, flexible design, and ability to precisely control the final state (see Fig. S10 in Supplemental Material [80]) in experiments.

In conclusion, we unveil a novel mechanism to achieve ultrafast magnetic-fieldless and currentless perpendicular magnetization switching by the voltage-controlled DMI torque in magnetoelectric multiferroics (e.g., $CuCrP_2Se_6$ and CrN). Through the accumulation of multiple skyrmion expansions, which are induced by the sign reversal of DMI with voltage pulses, the skyrmion in a limited geometry can continue to expand until it bursts into a quasiuniform FM state with reversed magnetization. Taking the size of a skyrmion as membrane potential and the alternating voltage pulse as input stimulus, we can also imitate the LIF operation of a biological neuron and achieve a skyrmion-based artificial neuron. The magnetization switching demonstrated in this Letter that is completely achieved through the voltage-induced DMI torque paves the way for alternative route to design skyrmion-based spintronic devices.

---

[*] cljia@lzu.edu.cn
[†] hongxin.yang@nju.edu.cn

[1] M. N. Baibich, J. M. Broto, A. Fert, F. N. Van Dau, F. Petroff, P. Etienne, G. Creuzet, A. Friederich, and J. Chazelas, Giant Magnetoresistance of (001)Fe/(001)Cr Magnetic Superlattices, Phys. Rev. Lett. **61**, 2472 (1988).

[2] G. Binasch, P. Grünberg, F. Saurenbach, and W. Zinn, Enhanced magnetoresistance in layered magnetic structures with antiferromagnetic interlayer exchange, Phys. Rev. B **39**, 4828 (1989).

[3] S. Yuasa, T. Nagahama, A. Fukushima, Y. Suzuki, and K. Ando, Giant room-temperature magnetoresistance in single-crystal Fe/MgO/Fe magnetic tunnel junctions, Nat. Mater. **3**, 868 (2004).

[4] S. S. P. Parkin, C. Kaiser, A. Panchula, P. M. Rice, B. Hughes, M. Samant, and S.-H. Yang, Giant tunnelling magnetoresistance at room temperature with MgO (100) tunnel barriers, Nat. Mater. **3**, 862 (2004).

[5] T. Song, X. Cai, W.-Y. Tu Matisse, X. Zhang, B. Huang, P. Wilson Nathan, L. Seyler Kyle, L. Zhu, T. Taniguchi, K. Watanabe, A. McGuire Michael, H. Cobden David, D. Xiao, W. Yao, and X. Xu, Giant tunneling magnetoresistance in spin-filter van der Waals heterostructures, Science **360**, 1214 (2018).

[6] C. Chappert, A. Fert, and F. N. Van Dau, The emergence of spin electronics in data storage, Nat. Mater. **6**, 813 (2007).

[7] J. C. Slonczewski, Current-driven excitation of magnetic multilayers, J. Magn. Magn. Mater. **159**, L1 (1996).

[8] L. Berger, Emission of spin waves by a magnetic multilayer traversed by a current, Phys. Rev. B **54**, 9353 (1996).

[9] A. D. Kent and D. C. Worledge, A new spin on magnetic memories, Nat. Nanotechnol. **10**, 187 (2015).

[10] D. Apalkov, B. Dieny, and J. M. Slaughter, Magnetoresistive random access memory, Proc. IEEE **104**, 1796 (2016).

[11] D. C. Ralph and M. D. Stiles, Spin transfer torques, J. Magn. Magn. Mater. **320**, 1190 (2008).

[12] M. D. Stiles and A. Zangwill, Anatomy of spin-transfer torque, Phys. Rev. B **66**, 014407 (2002).

[13] A. Manchon, J. Železný, I. M. Miron, T. Jungwirth, J. Sinova, A. Thiaville, K. Garello, and P. Gambardella,

Current-induced spin-orbit torques in ferromagnetic and antiferromagnetic systems, Rev. Mod. Phys. **91,** 035004 (2019).

[14] A. Hoffmann, Spin Hall effects in metals, IEEE Trans. Mag. **49,** 5172 (2013).

[15] A. Manchon and S. Zhang, Theory of nonequilibrium intrinsic spin torque in a single nanomagnet, Phys. Rev. B **78,** 212405 (2008).

[16] J. Sinova, S. O. Valenzuela, J. Wunderlich, C. H. Back, and T. Jungwirth, Spin Hall effects, Rev. Mod. Phys. **87,** 1213 (2015).

[17] A. Manchon, H. C. Koo, J. Nitta, S. M. Frolov, and R. A. Duine, New perspectives for Rashba spin–orbit coupling, Nat. Mater. **14,** 871 (2015).

[18] F. Hellman *et al.*, Interface-induced phenomena in magnetism, Rev. Mod. Phys. **89,** 025006 (2017).

[19] I. M. Miron, K. Garello, G. Gaudin, P.-J. Zermatten, M. V. Costache, S. Auffret, S. Bandiera, B. Rodmacq, A. Schuhl, and P. Gambardella, Perpendicular switching of a single ferromagnetic layer induced by in-plane current injection, Nature (London) **476,** 189 (2011).

[20] L. Liu, O. J. Lee, T. J. Gudmundsen, D. C. Ralph, and R. A. Buhrman, Current-Induced Switching of Perpendicularly Magnetized Magnetic Layers Using Spin Torque from the Spin Hall Effect, Phys. Rev. Lett. **109,** 096602 (2012).

[21] L. Liu, C.-F. Pai, Y. Li, H. W. Tseng, D. C. Ralph, and R. A. Buhrman, Spin-torque switching with the giant spin Hall effect of tantalum, Science **336,** 555 (2012).

[22] L. Liu, C. Zhou, X. Shu, C. Li, T. Zhao, W. Lin, J. Deng, Q. Xie, S. Chen, J. Zhou, R. Guo, H. Wang, J. Yu, S. Shi, P. Yang, S. Pennycook, A. Manchon, and J. Chen, Symmetry-dependent field-free switching of perpendicular magnetization, Nat. Nanotechnol. **16,** 277 (2021).

[23] I. M. Miron, T. Moore, H. Szambolics, L. D. Buda-Prejbeanu, S. Auffret, B. Rodmacq, S. Pizzini, J. Vogel, M. Bonfim, A. Schuhl, and G. Gaudin, Fast current-induced domain-wall motion controlled by the Rashba effect, Nat. Mater. **10,** 419 (2011).

[24] S. S. P. Parkin, K. P. Roche, M. G. Samant, P. M. Rice, R. B. Beyers, R. E. Scheuerlein, E. J. O'Sullivan, S. L. Brown, J. Bucchigano, D. W. Abraham, Y. Lu, M. Rooks, P. L. Trouilloud, R. A. Wanner, and W. J. Gallagher, Exchange-biased magnetic tunnel junctions and application to nonvolatile magnetic random access memory (invited), J. Appl. Phys. **85,** 5828 (1999).

[25] S. P. Parkin Stuart, M. Hayashi, and L. Thomas, Magnetic domain-wall racetrack memory, Science **320,** 190 (2008).

[26] K. Garello, F. Yasin, H. Hody, S. Couet, L. Souriau, S. H. Sharifi, J. Swerts, R. Carpenter, S. Rao, W. Kim, J. Wu, K. K. V. Sethu, M. Pak, N. Jossart, D. Crotti, A. Furnémont, and G. S. Kar, Manufacturable 300 mm platform solution for field-free switching SOT-MRAM, in *Symposium on VLSI Circuits* (IEEE, Kyoto, Japan, 2019), p. T194.

[27] K. Garello, F. Yasin, S. Couet, L. Souriau, J. Swerts, S. Rao, S. V. Beek, W. Kim, E. Liu, S. Kundu, D. Tsvetanova, K. Croes, N. Jossart, E. Grimaldi, M. Baumgartner, D. Crotti, A. Furnémont, P. Gambardella, and G. S. Kar,

SOT-MRAM 300MM integration for low power and ultrafast embedded memories, in *Symposium on VLSI Circuits* (IEEE, Honolulu, HI, 2018), p. 81.

[28] G. Prenat, K. Jabeur, P. Vanhauwaert, G. D. Pendina, F. Oboril, R. Bishnoi, M. Ebrahimi, N. Lamard, O. Boulle, K. Garello, J. Langer, B. Ocker, M. C. Cyrille, P. Gambardella, M. Tahoori, and G. Gaudin, Ultra-fast and high-reliability SOT-MRAM: From cache replacement to normally-off computing, IEEE Trans. Multi-Scale Comput. Syst. **2,** 49 (2016).

[29] M. Bibes and A. Barthélémy, Towards a magnetoelectric memory, Nat. Mater. **7,** 425 (2008).

[30] J. T. Heron, J. L. Bosse, Q. He, Y. Gao, M. Trassin, L. Ye, J. D. Clarkson, C. Wang, J. Liu, S. Salahuddin, D. C. Ralph, D. G. Schlom, J. Íñiguez, B. D. Huey, and R. Ramesh, Deterministic switching of ferromagnetism at room temperature using an electric field, Nature (London) **516,** 370 (2014).

[31] H. Béa, M. Bibes, F. Ott, B. Dupé, X. H. Zhu, S. Petit, S. Fusil, C. Deranlot, K. Bouzehouane, and A. Barthélémy, Mechanisms of Exchange Bias with Multiferroic BiFeO$_3$ Epitaxial Thin Films, Phys. Rev. Lett. **100,** 017204 (2008).

[32] Y.-H. Chu, L. W. Martin, M. B. Holcomb, M. Gajek, S.-J. Han, Q. He, N. Balke, C.-H. Yang, D. Lee, W. Hu, Q. Zhan, P.-L. Yang, A. Fraile-Rodríguez, A. Scholl, S. X. Wang, and R. Ramesh, Electric-field control of local ferromagnetism using a magnetoelectric multiferroic, Nat. Mater. **7,** 478 (2008).

[33] J. D. Burton and E. Y. Tsymbal, Prediction of electrically induced magnetic reconstruction at the manganite/ferroelectric interface, Phys. Rev. B **80,** 174406 (2009).

[34] S. Fusil, V. Garcia, A. Barthélémy, and M. Bibes, Magnetoelectric devices for spintronics, Annu. Rev. Mater. Res. **44,** 91 (2014).

[35] V. Garcia, M. Bibes, L. Bocher, S. Valencia, F. Kronast, A. Crassous, X. Moya, S. Enouz-Vedrenne, A. Gloter, D. Imhoff, C. Deranlot, N. D. Mathur, S. Fusil, K. Bouzehouane, and A. Barthélémy, Ferroelectric control of spin polarization, Science **327,** 1106 (2010).

[36] N. A. Spaldin and R. Ramesh, Advances in magnetoelectric multiferroics, Nat. Mater. **18,** 203 (2019).

[37] M. Gajek, M. Bibes, S. Fusil, K. Bouzehouane, J. Fontcuberta, A. Barthélémy, and A. Fert, Tunnel junctions with multiferroic barriers, Nat. Mater. **6,** 296 (2007).

[38] J. Wang, J. B. Neaton, H. Zheng, V. Nagarajan, S. B. Ogale, B. Liu, D. Viehland, V. Vaithyanathan, D. G. Schlom, U. V. Waghmare, N. A. Spaldin, K. M. Rabe, M. Wuttig, and R. Ramesh, Epitaxial BiFeO$_3$ multiferroic thin film heterostructures, Science **299,** 1719 (2003).

[39] C.-G. Duan, J. P. Velev, R. F. Sabirianov, Z. Zhu, J. Chu, S. S. Jaswal, and E. Y. Tsymbal, Surface Magnetoelectric Effect in Ferromagnetic Metal Films, Phys. Rev. Lett. **101,** 137201 (2008).

[40] J. P. Velev, C.-G. Duan, J. D. Burton, A. Smogunov, M. K. Niranjan, E. Tosatti, S. S. Jaswal, and E. Y. Tsymbal, Magnetic tunnel junctions with ferroelectric barriers:

Prediction of four resistance states from first principles, Nano Lett. **9,** 427 (2009).

[41] E. Y. Tsymbal, O. N. Mryasov, and P. R. LeClair, Spin-dependent tunnelling in magnetic tunnel junctions, J. Phys. Condens. Matter **15,** R109 (2003).

[42] I. Dzyaloshinsky, A thermodynamic theory of "weak" ferromagnetism of antiferromagnetics, J. Phys. Chem. Solids **4,** 241 (1958).

[43] T. Moriya, Anisotropic superexchange Interaction and weak ferromagnetism, Phys. Rev. **120,** 91 (1960).

[44] S. Heinze, K. von Bergmann, M. Menzel, J. Brede, A. Kubetzka, R. Wiesendanger, G. Bihlmayer, and S. Blügel, Spontaneous atomic-scale magnetic skyrmion lattice in two dimensions, Nat. Phys. **7,** 713 (2011).

[45] N. Romming, C. Hanneken, M. Menzel, E. Bickel Jessica, B. Wolter, K. von Bergmann, A. Kubetzka, and R. Wiesendanger, Writing and deleting single magnetic skyrmions, Science **341,** 636 (2013).

[46] O. Boulle, J. Vogel, H. Yang, S. Pizzini, D. de Souza Chaves, A. Locatelli, T. O. Menteş, A. Sala, L. D. Buda-Prejbeanu, O. Klein, M. Belmeguenai, Y. Roussigné, A. Stashkevich, S. M. Chérif, L. Aballe, M. Foerster, M. Chshiev, S. Auffret, I. M. Miron, and G. Gaudin, Room-temperature chiral magnetic skyrmions in ultrathin magnetic nanostructures, Nat. Nanotechnol. **11,** 449 (2016).

[47] C. Xu, P. Chen, H. Tan, Y. Yang, H. Xiang, and L. Bellaiche, Electric-Field Switching of Magnetic Topological Charge in Type-I Multiferroics, Phys. Rev. Lett. **125,** 037203 (2020).

[48] Q. H. Wang *et al.*, The magnetic genome of two-dimensional van der Waals materials, ACS Nano **16,** 6960 (2022).

[49] J. Liang, W. Wang, H. Du, A. Hallal, K. Garcia, M. Chshiev, A. Fert, and H. Yang, Very large Dzyaloshinskii-Moriya interaction in two-dimensional Janus manganese dichalcogenides and its application to realize skyrmion states, Phys. Rev. B **101,** 184401 (2020).

[50] G. Chen, M. Robertson, M. Hoffmann, C. Ophus, A. L. Fernandes Cauduro, R. Lo Conte, H. Ding, R. Wiesendanger, S. Blügel, A. K. Schmid, and K. Liu, Observation of Hydrogen-Induced Dzyaloshinskii-Moriya Interaction and Reversible Switching of Magnetic Chirality, Phys. Rev. X **11,** 021015 (2021).

[51] J. Liang, Q. Cui, and H. Yang, Electrically switchable Rashba-type Dzyaloshinskii-Moriya interaction and skyrmion in two-dimensional magnetoelectric multiferroics, Phys. Rev. B **102,** 220409(R) (2020).

[52] H. Yang, J. Liang, and Q. Cui, First-principles calculations for Dzyaloshinskii–Moriya interaction, Nat. Rev. Phys. **5,** 43 (2023).

[53] A. Thiaville, S. Rohart, É. Jué, V. Cros, and A. Fert, Dynamics of Dzyaloshinskii domain walls in ultrathin magnetic films, Europhys. Lett. **100,** 57002 (2012).

[54] K.-S. Ryu, L. Thomas, S.-H. Yang, and S. Parkin, Chiral spin torque at magnetic domain walls, Nat. Nanotechnol. **8,** 527 (2013).

[55] M. Heide, G. Bihlmayer, and S. Blügel, Dzyaloshinskii-Moriya interaction accounting for the orientation of magnetic domains in ultrathin films: Fe/W(110), Phys. Rev. B **78,** 140403(R) (2008).

[56] J. Sampaio, V. Cros, S. Rohart, A. Thiaville, and A. Fert, Nucleation, stability and current-induced motion of isolated magnetic skyrmions in nanostructures, Nat. Nanotechnol. **8,** 839 (2013).

[57] X. Z. Yu, Y. Onose, N. Kanazawa, J. H. Park, J. H. Han, Y. Matsui, N. Nagaosa, and Y. Tokura, Real-space observation of a two-dimensional skyrmion crystal, Nature (London) **465,** 901 (2010).

[58] A. Fert, N. Reyren, and V. Cros, Magnetic skyrmions: advances in physics and potential applications, Nat. Rev. Mater. **2,** 17031 (2017).

[59] S. Mühlbauer, B. Binz, F. Jonietz, C. Pfleiderer, A. Rosch, A. Neubauer, R. Georgii, and P. Böni, Skyrmion lattice in a chiral magnet, Science **323,** 915 (2009).

[60] X. Z. Yu, N. Kanazawa, Y. Onose, K. Kimoto, W. Z. Zhang, S. Ishiwata, Y. Matsui, and Y. Tokura, Near room-temperature formation of a skyrmion crystal in thin-films of the helimagnet FeGe, Nat. Mater. **10,** 106 (2011).

[61] W. Jiang, P. Upadhyaya, W. Zhang, G. Yu, M. B. Jungfleisch, Y. Fradin Frank, E. Pearson John, Y. Tserkovnyak, L. Wang Kang, O. Heinonen, G. E. te Velthuis Suzanne, and A. Hoffmann, Blowing magnetic skyrmion bubbles, Science **349,** 283 (2015).

[62] W. Jiang, X. Zhang, G. Yu, W. Zhang, X. Wang, M. Benjamin Jungfleisch, John E. Pearson, X. Cheng, O. Heinonen, K. L. Wang, Y. Zhou, A. Hoffmann, and Suzanne G. E. te Velthuis, Direct observation of the skyrmion Hall effect, Nat. Phys. **13,** 162 (2017).

[63] J. Iwasaki, M. Mochizuki, and N. Nagaosa, Current-induced skyrmion dynamics in constricted geometries, Nat. Nanotechnol. **8,** 742 (2013).

[64] K. Huang, D.-F. Shao, and E. Y. Tsymbal, Ferroelectric control of magnetic skyrmions in two-dimensional van der Waals heterostructures, Nano Lett. **22,** 3349 (2022).

[65] T. Srivastava, M. Schott, R. Juge, V. Křižáková, M. Belmeguenai, Y. Roussigné, A. Bernand-Mantel, L. Ranno, S. Pizzini, S.-M. Chérif, A. Stashkevich, S. Auffret, O. Boulle, G. Gaudin, M. Chshiev, C. Baraduc, and H. Béa, Large-voltage tuning of Dzyaloshinskii–Moriya interactions: A route toward dynamic control of skyrmion chirality, Nano Lett. **18,** 4871 (2018).

[66] H. Yang, A. Thiaville, S. Rohart, A. Fert, and M. Chshiev, Anatomy of Dzyaloshinskii-Moriya Interaction at Co/Pt Interfaces, Phys. Rev. Lett. **115,** 267210 (2015).

[67] N. Nagaosa and Y. Tokura, Topological properties and dynamics of magnetic skyrmions, Nat. Nanotechnol. **8,** 899 (2013).

[68] J. Qi, H. Wang, X. Chen, and X. Qian, Two-dimensional multiferroic semiconductors with coexisting ferroelectricity and ferromagnetism, Appl. Phys. Lett. **113,** 043102 (2018).

[69] W. Luo, K. Xu, and H. Xiang, Two-dimensional hyperferroelectric metals: A different route to ferromagnetic-ferroelectric multiferroics, Phys. Rev. B **96,** 235415 (2017).

[70] Z. Shao, J. Liang, Q. Cui, M. Chshiev, A. Fert, T. Zhou, and H. Yang, Multiferroic materials based on transition-metal dichalcogenides: Potential platform for reversible control of Dzyaloshinskii-Moriya interaction and skyrmion via electric field, Phys. Rev. B **105,** 174404 (2022).

[71] S. Rohart and A. Thiaville, Skyrmion confinement in ultrathin film nanostructures in the presence of Dzyaloshinskii-Moriya interaction, Phys. Rev. B **88,** 184422 (2013).

[72] W. Maass, Networks of spiking neurons: The third generation of neural network models, Neural Netw. **10,** 1659 (1997).

[73] J. Grollier, D. Querlioz, K. Y. Camsari, K. Everschor-Sitte, S. Fukami, and M. D. Stiles, Neuromorphic spintronics, Nat. Electron. **3,** 360 (2020).

[74] J. Torrejon, M. Riou, F. A. Araujo, S. Tsunegi, G. Khalsa, D. Querlioz, P. Bortolotti, V. Cros, K. Yakushiji, A. Fukushima, H. Kubota, S. Yuasa, M. D. Stiles, and J. Grollier, Neuromorphic computing with nanoscale spintronic oscillators, Nature (London) **547,** 428 (2017).

[75] M. Romera, P. Talatchian, S. Tsunegi, F. Abreu Araujo, V. Cros, P. Bortolotti, J. Trastoy, K. Yakushiji, A. Fukushima, H. Kubota, S. Yuasa, M. Ernoult, D. Vodenicarevic, T. Hirtzlin, N. Locatelli, D. Querlioz, and J. Grollier, Vowel recognition with four coupled spin-torque nano-oscillators, Nature (London) **563,** 230 (2018).

[76] K. M. Song, J.-S. Jeong, B. Pan, X. Zhang, J. Xia, S. Cha, T.-E. Park, K. Kim, S. Finizio, J. Raabe, J. Chang, Y. Zhou, W. Zhao, W. Kang, H. Ju, and S. Woo, Skyrmion-based artificial synapses for neuromorphic computing, Nat. Electron. **3,** 148 (2020).

[77] X. Liang, X. Zhang, J. Xia, M. Ezawa, Y. Zhao, G. Zhao, and Y. Zhou, A spiking neuron constructed by the skyrmion-based spin torque nano-oscillator, Appl. Phys. Lett. **116,** 122402 (2020).

[78] J. Chu, Y. Wang, X. Wang, K. Hu, G. Rao, C. Gong, C. Wu, H. Hong, X. Wang, K. Liu, C. Gao, and J. Xiong, 2D polarized materials: Ferromagnetic, ferrovalley, ferroelectric materials, and related heterostructures, Adv. Mater. **33,** 2004469 (2021).

[79] X. Wang, Z. Song, W. Wen, H. Liu, J. Wu, C. Dang, M. Hossain, M. A. Iqbal, and L. Xie, Potential 2D materials with phase transitions: Structure, synthesis, and device applications, Adv. Mater. **31,** 1804682 (2019).

[80] See Supplemental Material at http://link.aps.org/supplemental/10.1103/PhysRevLett.130.056701 for more details about the DFT method and parameters, micromagnetic simulations, and skyrmion-based artificial neuron, as well as the theoretical analysis of the skyrmion expansion, which includes Refs. [51,67,74–77,81–94].

[81] G. Kresse and J. Furthmüller, Efficient iterative schemes for *ab initio* total-energy calculations using a plane-wave basis set, Phys. Rev. B **54,** 11169 (1996).

[82] J. P. Perdew, K. Burke, and M. Ernzerhof, Generalized Gradient Approximation Made Simple, Phys. Rev. Lett. **77,** 3865 (1996).

[83] G. Kresse and J. Hafner, *Ab initio* molecular dynamics for liquid metals, Phys. Rev. B **47,** 558 (1993).

[84] G. Kresse and J. Hafner, *Ab initio* molecular-dynamics simulation of the liquid-metal–amorphous-semiconductor transition in germanium, Phys. Rev. B **49,** 14251 (1994).

[85] G. Kresse and J. Furthmüller, Efficiency of *ab-initio* total energy calculations for metals and semiconductors using a plane-wave basis set, Comput. Mater. Sci. **6,** 15 (1996).

[86] L. M. Sandratskii, Insight into the Dzyaloshinskii-Moriya interaction through first-principles study of chiral magnetic structures, Phys. Rev. B **96,** 024450 (2017).

[87] M. Heide, G. Bihlmayer, and S. Blügel, Describing Dzyaloshinskii–Moriya spirals from first principles, Physica (Amsterdam) **404B,** 2678 (2009).

[88] H. Jaffrès, D. Lacour, F. Nguyen Van Dau, J. Briatico, F. Petroff, and A. Vaurès, Angular dependence of the tunnel magnetoresistance in transition-metal-based junctions, Phys. Rev. B **64,** 064427 (2001).

[89] D. M. Crum, M. Bouhassoune, J. Bouaziz, B. Schweflinghaus, S. Blügel, and S. Lounis, Perpendicular reading of single confined magnetic skyrmions, Nat. Commun. **6,** 8541 (2015).

[90] R. F. L. Evans, W. J. Fan, P. Chureemart, T. A. Ostler, M. O. A. Ellis, and R. W. Chantrell, Atomistic spin model simulations of magnetic nanomaterials, J. Phys. Condens. Matter **26,** 103202 (2014).

[91] X. S. Wang, H. Y. Yuan, and X. R. Wang, A theory on skyrmion size, Commun. Phys. **1,** 31 (2018).

[92] L. Landau and E. Lifshitz, in *Perspectives in Theoretical Physics*, edited by L. P. Pitaevski (Pergamon, Amsterdam, 1992), p. 51.

[93] J. Chen and S. Dong, Manipulation of Magnetic Domain Walls by Ferroelectric Switching: Dynamic Magnetoelectricity at the Nanoscale, Phys. Rev. Lett. **126,** 117603 (2021).

[94] F. H. D. Leeuw, R. V. D. Doel, and U. Enz, Dynamic properties of magnetic domain walls and magnetic bubbles, Rep. Prog. Phys. **43,** 689 (1980).

[95] Y. Onose, Y. Okamura, S. Seki, S. Ishiwata, and Y. Tokura, Observation of Magnetic Excitations of Skyrmion Crystal in a Helimagnetic Insulator Cu_2OSeO_3, Phys. Rev. Lett. **109,** 037603 (2012).

[96] Y. Zhou, E. Iacocca, A. A. Awad, R. K. Dumas, F. C. Zhang, H. B. Braun, and J. Åkerman, Dynamically stabilized magnetic skyrmions, Nat. Commun. **6,** 8193 (2015).

[97] K. Zeissler, S. Finizio, C. Barton, A. J. Huxtable, J. Massey, J. Raabe, A. V. Sadovnikov, S. A. Nikitov, R. Brearton, T. Hesjedal, G. van der Laan, M. C. Rosamond, E. H. Linfield, G. Burnell, and C. H. Marrows, Diameter-independent skyrmion Hall angle observed in chiral magnetic multilayers, Nat. Commun. **11,** 428 (2020).

[98] K. Zeissler, S. Finizio, K. Shahbazi, J. Massey, F. A. Ma'Mari, D. M. Bracher, A. Kleibert, M. C. Rosamond, E. H. Linfield, T. A. Moore, J. Raabe, G. Burnell, and C. H. Marrows, Discrete Hall resistivity contribution from Néel skyrmions in multilayer nanodiscs, Nat. Nanotechnol. **13,** 1161 (2018).

[99] K. Zeissler, M. Mruczkiewicz, S. Finizio, J. Raabe, P. M. Shepley, A. V. Sadovnikov, S. A. Nikitov, K. Fallon, S. McFadzean, S. McVitie, T. A. Moore, G. Burnell, and C. H. Marrows, Pinning and hysteresis in the field dependent diameter evolution of skyrmions in Pt/Co/Ir superlattice stacks, Sci. Rep. **7,** 15125 (2017).

[100] J. T. Heron, M. Trassin, K. Ashraf, M. Gajek, Q. He, S. Y. Yang, D. E. Nikonov, Y. H. Chu, S. Salahuddin, and R. Ramesh, Electric-Field-Induced Magnetization Reversal in a Ferromagnet-Multiferroic Heterostructure, Phys. Rev. Lett. **107,** 217202 (2011).

[101] M. Liu and N. X. Sun, Voltage control of magnetism in multiferroic heterostructures, Phil. Trans. R. Soc. A **372**, 20120439 (2014).

[102] M. Liu, J. Lou, S. Li, and N. X. Sun, E-field control of exchange bias and deterministic magnetization switching in AFM/FM/FE multiferroic heterostructures, Adv. Funct. Mater. **21**, 2593 (2011).

[103] M. Fechner, P. Zahn, S. Ostanin, M. Bibes, and I. Mertig, Switching Magnetization by 180° with an Electric Field, Phys. Rev. Lett. **108**, 197206 (2012).

[104] W. Koshibae and N. Nagaosa, Creation of skyrmions and antiskyrmions by local heating, Nat. Commun. **5**, 5148 (2014).

[105] D. Bhattacharya, M. M. Al-Rashid, and J. Atulasimha, Voltage controlled core reversal of fixed magnetic skyrmions without a magnetic field, Sci. Rep. **6**, 31272 (2016).

[106] T. A. Ostler, R. Cuadrado, R. W. Chantrell, A. W. Rushforth, and S. A. Cavill, Strain Induced Vortex Core Switching in Planar Magnetostrictive Nanostructures, Phys. Rev. Lett. **115**, 067202 (2015).